

## Effect of Frontal Plane Tibiofemoral Angle on the Stress and Strain at the Knee Cartilage During the Stance Phase of Gait

Nicholas H. Yang,<sup>1</sup> Hamid Nayeb-Hashemi,<sup>1</sup> Paul K. Canavan,<sup>2</sup> Ashkan Vaziri<sup>1</sup>

<sup>1</sup>Department of Mechanical and Industrial Engineering, Northeastern University, Boston, Massachusetts, <sup>2</sup>Department of Physical Therapy, Northeastern University, Boston, Massachusetts

Received 12 August 2009; accepted 22 March 2010

Published online in Wiley InterScience (www.interscience.wiley.com). DOI 10.1002/jor.21174

**ABSTRACT:** Subject-specific three-dimensional finite element models of the knee joint were created and used to study the effect of the frontal plane tibiofemoral angle on the stress and strain distribution in the knee cartilage during the stance phase of the gait cycle. Knee models of three subjects with different tibiofemoral angle and body weight were created based on magnetic resonance imaging of the knee. Loading and boundary conditions were determined from motion analysis and force platform data, in conjunction with the muscle-force reduction method. During the stance phase of walking, all subjects exhibited a valgus–varus–valgus knee moment pattern with the maximum compressive load and varus knee moment occurring at approximately 25% of the stance phase of the gait cycle. Our results demonstrated that the subject with varus alignment had the largest stresses at the medial compartment of the knee compared to the subjects with normal alignment and valgus alignment, suggesting that this subject might be most susceptible to developing medial compartment osteoarthritis (OA). In addition, the magnitude of stress and strain on the lateral cartilage of the subject with valgus alignment were found to be larger compared to subjects with normal alignment and varus alignment, suggesting that this subject might be most susceptible to developing lateral compartment knee OA. © 2010 Orthopaedic Research Society. Published by Wiley Periodicals, Inc. *J. Orthop. Res.* 9999: 1–9, 2010

**Keywords:** knee biomechanics; subject-specific model; motion analysis; finite-element method; tibiofemoral angle; varus/valgus

### INTRODUCTION

Knee malalignment is considered one of the key biomechanical factors that influence the progression of knee osteoarthritis (OA).<sup>1,2</sup> The frontal plane tibiofemoral alignment at the knee is measured by the angle formed by the intersection of the anatomical axes of the femur and the tibia. A “normal” knee alignment has a tibiofemoral angle of approximately 5–7° valgus.<sup>3,4</sup> A varus-aligned knee is described as “bow-legged” with an angle <5° valgus and a valgus-aligned knee is described as “knocked-kneed” with an angle >7° valgus. The varus (adduction) moment is the primary factor in the force distribution to the medial compartment of the knee joint during normal gait. During walking, approximately 70–75% of the load passes to the medial compartment of the knee joint.<sup>5,6</sup> At the single-leg support phase of the gait cycle, a varus-aligned knee will have a moment that increases the loading on the medial compartment of the knee and a valgus-aligned knee will have a moment that increases the loading on the lateral compartment of the knee. However, in individuals with extremely malaligned valgus knees (15° valgus), the lateral knee compartment will experience more load than the medial knee compartment.<sup>2,4</sup> In longitudinal studies, from baseline assessment, individuals who demonstrated a varus knee alignment were shown to have an increase in medial compartment OA pro-

gression and valgus knee alignment was shown to have an increase in lateral OA progression in as little as 18 months.<sup>7</sup> It is not entirely clear if varus/valgus alignment is a cause or a result of knee OA, but animal data supports a link between pre-existing varus/valgus alignment and OA initiation.<sup>7,8</sup> Furthermore, the increased stress and strain caused by the varus moment due to alignment could contribute to the initiation and progression of OA and has not been previously investigated.

Direct measurement of stress and strain at the knee cartilage in vivo is challenging, therefore the finite element (FE) method has been used to determine the stresses and strains within the knee.<sup>9–12</sup> Previously developed FE knee models provide significant insight into the stress and strain distribution and contact kinematics at the knee joint and have been used to investigate the effect of ligament injury<sup>13,14</sup> and meniscectomy<sup>15,16</sup> on the contact stress and strain at the knee cartilage. However, many FE studies apply simple loading conditions and do not consider subject-specific physiological loading during functional activities which would provide a more realistic representation of the actual stresses and strains within the knee joint.

In the present study, the effect of frontal plane tibiofemoral angle on the distribution of stresses and strains in the knee cartilage was investigated using detailed subject-specific FE models. We developed subject-specific biomechanical FE models of the knee joint for three subjects with normal, varus, and valgus tibiofemoral alignment and used the models to monitor the distribution of stresses and strains during the entire stance phase of the gait cycle. It was hypothesized that varus knee alignment will lead to greater

Additional supporting information may be found in the online version of this article.

Correspondence to: Nicholas H. Yang (T: 1-617-373-3474<sup>AQ2</sup>; E-mail: nhyang@coe.neu.edu)

© 2010 Orthopaedic Research Society. Published by Wiley Periodicals, Inc.

**Table 1.** Subjects' Frontal Plane Tibiofemoral Angle and Body Weight

Subject	1 (Varus)	2 (Normal)	3 (Valgus)
Tibiofemoral angle valgus (°)	0.20	7.67	10.34
Body weight (N)	640	725	704

varus knee moments which will lead to greater stresses at the medial knee compartment during the gait cycle and possibly increase the likelihood of OA initiation and progression.

## METHODS

Three healthy individuals with no history of knee OA or prior knee injury were recruited from the Northeastern University community. The subjects consisted of one male and two females (21- to 23-year old) with different frontal plane tibiofemoral angle (normal, varus, valgus). The frontal plane tibiofemoral angle was measured while the subjects were in a double leg-stance position with each leg on a separate force plate (while monitoring the force to ensure an even weight distribution between each leg) with the second metatarsal of the 2 feet approximately 30 cm apart. The anatomical axis of the femur in the frontal plane was defined with the marker at the ASIS and the knee-joint center. The hip joint center has been measured in a noninvasive manner by taking the midpoint of the line from the ASIS to the pubic symphysis and move inferiorly 2 cm.<sup>17</sup> A marker placed just lateral to the palpable femoral pulse approximately 2–3 cm below the inguinal ligament is suitable as a guide to locate the center of the femoral head when determining the mechanical axis during total knee arthroplasty.<sup>18</sup> In the current study, the hip joint center was defined using markers placed at the ASIS and the greater trochanter. A more accurate definition of the hip joint center would be necessary to determine the hip joint kinematics, however, those were not calculated in this investigation. The anatomical axis of the tibia was defined from the ankle joint center to the knee-joint center, similar to previous studies which used markers and motion analysis to define the frontal plane angle.<sup>19</sup> The tibiofemoral angle was assessed while the subjects were in this standard double-leg stance to ensure minimal rotation of the tibia.<sup>5</sup> The measurement of the tibiofemoral angle of the three subjects showed a varus individual (subject 1), normal (slightly valgus) individual (subject 2), and a valgus individual (subject 3; Table 1).

Subject-specific three-dimensional (3D) knee models were constructed from sagittal view magnetic resonance images (MRI). The MRI were obtained using a short bore, high-field 1.5 Tesla MRI device and a fat suppressed fast spin echo sequence with a with TE = 10 ms, TR = 536 ms, 160 mm × 160 mm field of view and slice thickness of 2 mm with 256 × 256 matrix and approximately 50 images. The 3D knee geometry was exported to ABAQUS v 6.7 (Simulia, Providence, RI), which was used to perform the FE simulations. The details for development of subject-specific models, including the material models used to represent the behavior of different knee elements, are demonstrated in the Supporting Material. The bone in the model included the femur, tibia and fibula with the corresponding cartilage on the femur and tibia. The cartilage was modeled as isotropic elastic and the meniscus as transversely isotropic elastic. The medial and lateral menisci were also included as

well as the anterior cruciate ligament (ACL), posterior cruciate ligament (PCL), lateral collateral ligament (LCL), and the medial collateral ligament (MCL).

Subject-specific loading at the knee was determined from motion analysis and force platform data and a muscle-force reduction model. Retro-reflective markers were placed at bony landmarks to define the different segments of the lower leg. Kinematics and kinetic data were collected with a six-camera motion analysis system (EVA<sup>RT</sup> 5.0, Motion Analysis Corporation, Santa Rosa, CA) and two-force platforms (Models OR6-6-2000, OR6-7-2000; Advanced Mechanical Technology, Inc. (AMTI), Waltham, MA), respectively. The motion analysis cameras recorded at a frequency of 120 Hz over a capture volume of 1.15 m × 2.00 m × 2.00 m. Two-force platforms were used for recording the ground reaction forces at a frequency of 1,200 Hz and were time synchronized with the motion analysis system. The ground reaction forces and center of pressure (COP) were measured by the force platforms. The measurements in this system were accurate within 2 mm.<sup>20</sup>

Subjects performed three trials of walking at a self-selected speed while monitoring the ground reaction forces and the kinematics of one leg. We preferred to use over ground walking with self-selected speed to screen natural functioning of the knee, therefore, treadmills and timing techniques to control speed were not used. Our previous investigations suggest that the inter-cycle gait variability during self-selected speed is low in healthy subjects (<2% for coefficient of variation of gait speed).<sup>21–23</sup> An inverse dynamics analysis was used to calculate the knee-joint reactions forces and moments as explained in our previous study.<sup>24</sup> To calculate the contribution of the muscle forces, a muscle-force reduction model was used similar to previous studies by Morrison<sup>25</sup> and Schipplein and Andriacchi.<sup>26</sup> The forces applied to the FE models were a summation of the joint reactions forces and the muscle forces. Figure 1 shows the total axial force and anterior/posterior force for a typical subject and the contributions from the ground reaction forces and muscle forces. The time history loading conditions were applied to the femur to define the knee forces during the stance phase of the gait cycle. The loading conditions applied to the model included the axial force  $F_z$ , the anterior/posterior force  $F_y$ , and the varus/valgus moment  $M_x$  and the internal/external rotation moment  $M_z$ . The flexion/extension moment  $M_y$  was not directly applied to the model but the knee-flexion angle was defined with an angular velocity, which was determined as the time derivative of the flexion angle during the stance phase of the gait cycle.

The moments at the knee were divided by the subject-specific body mass to define the normalized varus/valgus knee moment to account for the different body weights of the subjects. Similarly, results from the FE models were divided by subject-specific body weight to define the normalized stress and strain to account for the different body weight of the subjects and to view the role of the tibiofemoral angle.

## RESULTS

The inverse dynamics analysis and muscle-force reduction models showed each subject had different joint reaction forces and moments. As an example, Figure 2A and B shows the history of the axial and anterior/posterior reaction forces during the stance phase of the gait cycle for the three subjects. The different peaks demonstrate the activation of the different muscles where the first peak was activation of the hamstrings,

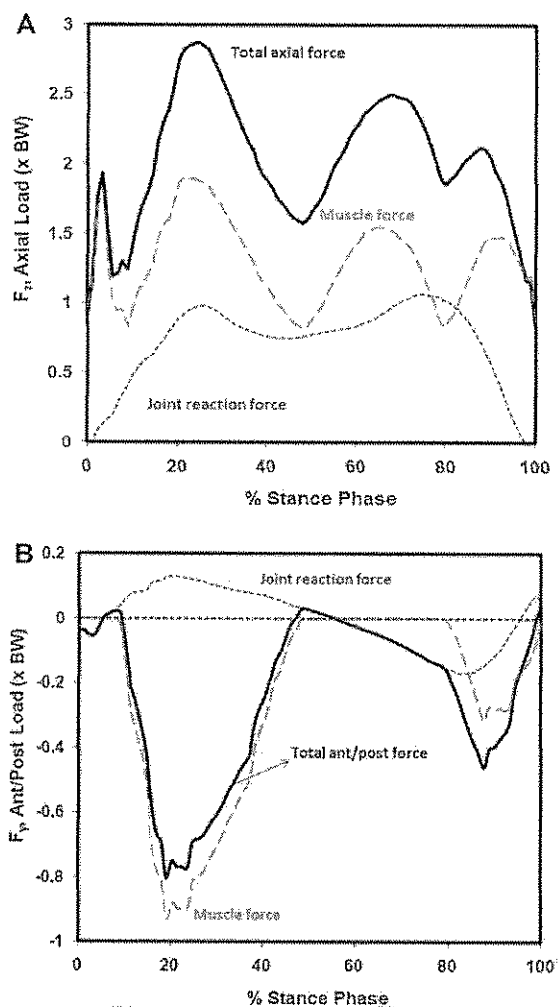


**Figure 1.** The total force, muscle force contribution and joint reaction force contribution in multiples of body weight (BW) in the (A) vertical direction,  $F_z$ , and the (B) anterior/posterior direction,  $F_y$ , during the stance phase of the gait cycle for Subject 1 (varus).

the second and fourth peaks were the quadriceps and the third peak was the gastrocnemius muscle group. Figure 2C shows the time history of varus/valgus knee moment during one gait cycle for three subjects. Of particular interest is the varus knee moment distribution because it is key factor in the force distribution at the knee and increased tibiofemoral alignment was expected to lead to greater force distributed to the medial knee compartment. Comparing the varus/valgus knee moment during the stance phase of the gait cycle showed that Subject 1 (varus alignment) exhibited a larger varus knee moment during single-leg support compared to Subjects 2 (relative normal alignment) and 3 (valgus alignment). The maximum varus knee moment was normalized by subject-specific body mass and was 0.49,

0.37, and 0.34 N m/kg for Subjects 1, 2, and 3, respectively.

FE analysis was carried out to obtain the distribution of the stresses and strains in the knee-joint cartilages during the gait cycle using detailed subject-specific models. Figure 3 shows a typical distribution of compressive stresses in the femoral cartilage, meniscus, and tibial cartilage at different points of the gait cycle (Subject 2). At heel-strike, the subject had an initial valgus moment and this caused the maximum compressive stress in the cartilage to occur on the lateral knee compartment. During the single-leg support phase of the stance phase, the subject exhibited a varus moment and the maximum compressive stress in the cartilage occurred on the medial knee compartment. At toe-off, there was a valgus knee moment and the maximum compressive stress occurred on the lateral compartment. Similar results were observed for both the maximum shear stress (Tresca stress) and the normal strain. The results clearly show the role of the varus/valgus knee moment in determining the location of maximum stress on either the medial or lateral knee compartment during the gait cycle. The maximum compressive stress on the knee cartilage for each subject at different points of the gait cycle is quantified in Figure 4. For each subject, at a valgus knee moment (heel strike to foot flat, first 10% of stance phase and toe off or 95% of the stance phase) the maximum compressive stress occurred on the lateral compartment of the knee. From 25% to 75% of the stance phase (i.e., during the varus moment), the maximum compressive stress occurred on the medial knee compartment. Furthermore, the peak maximum stress occurred on the medial cartilage at 25% of the stance phase of the gait cycle for each subject, which is associated with the peak varus knee moment for each subject—see Figure 2. The distribution of the compressive stress and Tresca shear stress, Figure 5, showed that the maximum values occurred on the medial cartilage for each subject. The greatest value of the normalized maximum compressive stress (normalized by the subject-specific body weight), normalized maximum Tresca shear stress, and normal strain occurred at 25% of the stance phase and increased with increased varus alignment as quantified in Table 2. At 25% of the stance phase, Subject 1 (varus) had greater values of the maximum normalized compressive stress, normalized shear stress, and normal strain compared to Subjects 2 (normal) and 3 (valgus). The greatest difference occurred for the normal strain at the femoral cartilage where Subject 1 had a 20% greater strain than Subject 2 and a 39% greater strain than Subject 3.

We also determined the ligament forces in the ACL, PCL, LCL, and MCL during the stance phase of the gait cycle for each subject using our FE calculations. Figure 6 shows the ligament forces for each subject during a specific trial of the stance phase of the gait cycle for each subject. The largest force occurred in the ACL and LCL. The maximum force in the ACL was approximately 350 N for Subject 1 (varus), 500 N for Subject

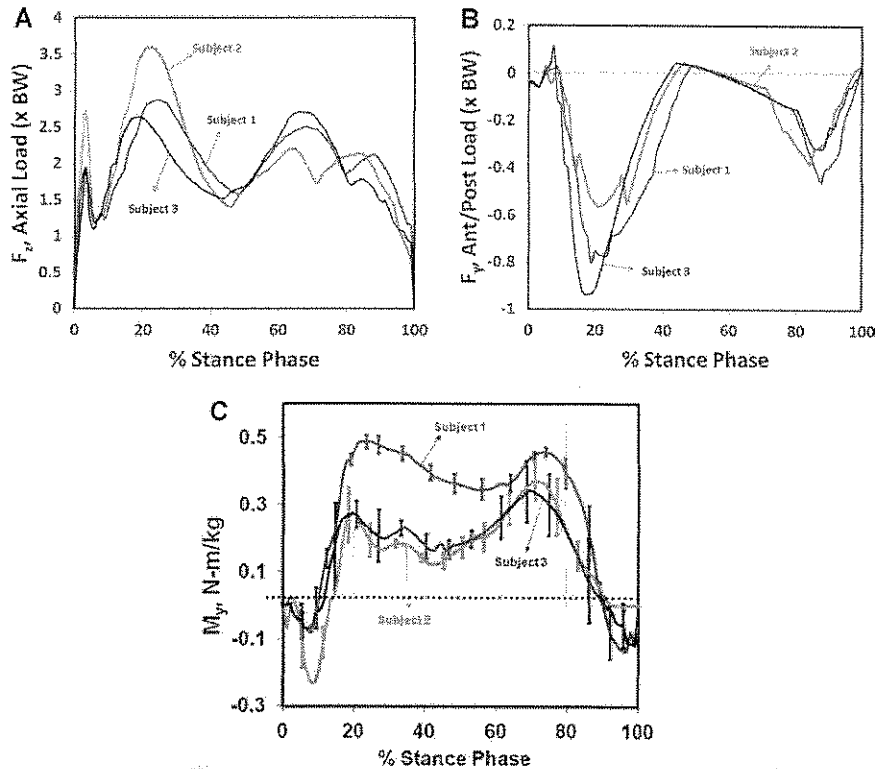


**Figure 2.** (A) Total compressive force,  $F_z$ , (B) total anterior/posterior shear force,  $F_y$ , and (C) mean varus/valgus knee moment,  $M_y$ , for Subject 1 (varus alignment), Subject 2 (relative normal), and Subject 3 (valgus alignment) during the stance phase (heel-strike to toe-off) of the gait cycle. (C) Varus/valgus knee moment and standard deviation for three trials of gait. A positive moment is varus and a negative moment is valgus.

2 (normal alignment), and 300 N for Subject 3 (valgus). The maximum force in the LCL for Subject 1 occurred at approximately mid-stance and was 350 N, at 25% of the stance phase and approximately 375 N for Subject 2, and at heel-strike and 200 N for Subject 3.

## DISCUSSION

In this study, we used subject-specific 3D models of the knee joints to explore the effect of the frontal plane tibiofemoral angle on the stress and strain at the knee cartilage during the stance phase of the gait cycle. Studying the compressive stress and strain is of interest because experimental studies have related cartilage damage with the magnitude of the compressive stress and strain.<sup>27,28</sup> Shear stress has also been associated with increased catabolic factors and decreased cartilage biosynthetic activity and leads to cartilage damage and subsequent OA.<sup>13</sup> The results showed the maximum value of the stress and strain occurred at 25% of the stance phase which is when the initial peak varus knee moment occurred. This could explain why the initial peak varus knee moment has been shown to be a predictor of the presence, severity, and rate of progression in knee OA on the medial compartment.<sup>29</sup> The results

also showed increased varus knee alignment led to greater varus knee moments during single-leg support. The results agree with our hypothesis that increased varus knee moment led to greater stresses and strain on the medial knee compartment for the varus-aligned individual compared to the normal-aligned and valgus-aligned subjects, suggesting that Subject 1 (varus) would be most susceptible to developing medial compartment knee OA. It is apparent that the increased varus moment generated in varus tibiofemoral aligned individuals would create larger forces at the medial knee compartment compared to normal-aligned individuals or valgus-aligned individuals. However, FE results provide important information on the stress and strain distribution at the knee cartilage for each individual that cannot be obtained with motion analysis techniques alone.

To replicate the subject's gait outdoors and in natural environment, we used over ground walking with self-selecting speed. Gait speed could contribute to the overall magnitude of the forces at the knee during gait. Although by using instrumented treadmills the gait speed can be controlled, uncertainty remains regarding the extent to which treadmill walking can be used

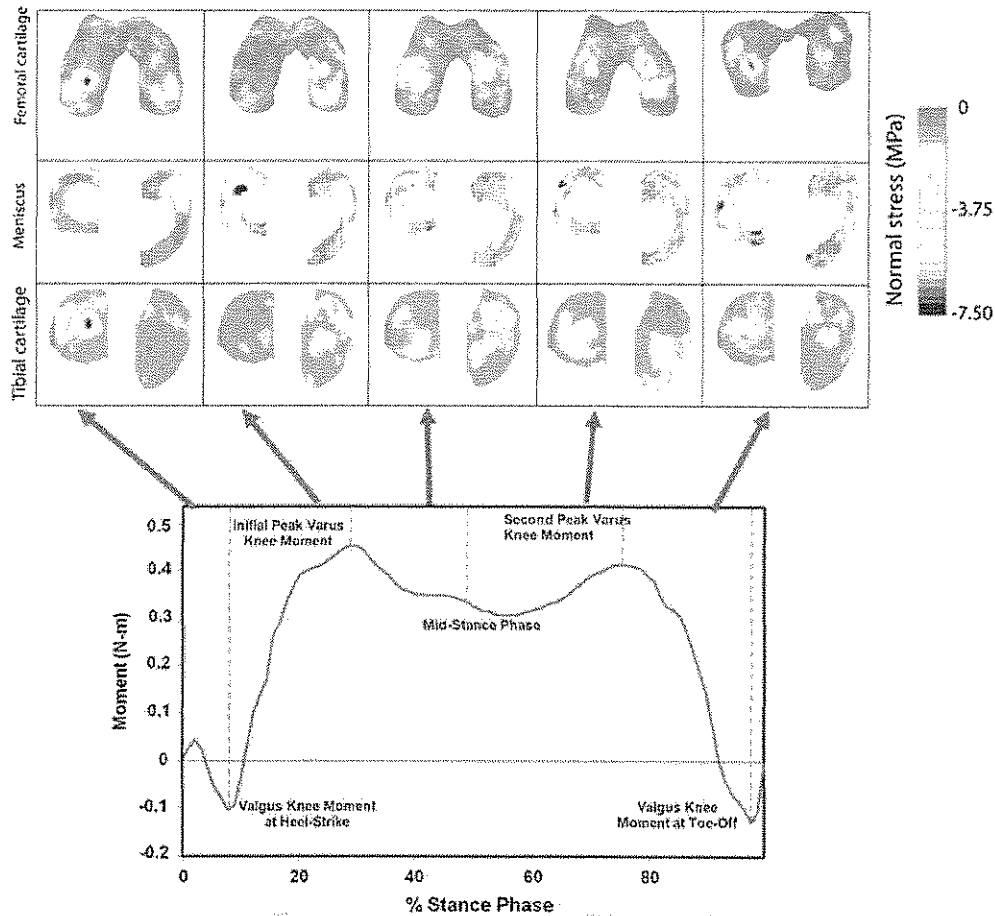


**Figure 3.** Finite element results from Subject 2 (normal alignment). The varus/valgus knee moment during the stance phase of the gait cycle determined from inverse dynamics analysis. Compressive stress distribution of femoral cartilage and tibial plateau (meniscus and tibial cartilage) of the right knee corresponding to specific amounts of the varus/valgus knee moment. In all the images, the medial side is on the left and the lateral side is on the right.

to mimic walking on the ground.<sup>21,30</sup> In addition, the narrow path offered by the treadmill as well as small freedom for inter-cycle speed variability may hinder freedom in selection of gait trajectory and/or speed. This in turn may impact the functioning of knee joint, which is hard to control. This suggests that the fluctuation of self-selected gait speed during over ground walking is low, therefore, the functioning of knee assessed in a typical cycle and in natural condition could be representative of knee functioning of subject's gait in daily condition. However, walking slower or faster than self-selected speed may significantly increase subject's gait inter-cycle fluctuations<sup>19-21</sup> and may not replicate subject's knee functioning during daily activity.

To show the validity of the current model, the magnitude of the ligament forces calculated in the current model agreed with previously published studies.<sup>25,31,32</sup> The material models of the ligaments were taken from

previously published studies and changes in the pre-strain of the ligaments may change the overall contact forces as well as the forces in the ligaments. The maximum value in the ACL computed by Morrison<sup>25</sup> was 156 N, in a mathematical model, 303 N calculated by Shelburne et al.<sup>31</sup> in a 3D computer model and 411 N by Harrington<sup>32</sup> in a mathematical model. The maximum load in the LCL computed by Morrison<sup>25</sup> was 262 N and Shelburne et al.<sup>31</sup> calculated 150 N. Our maximum LCL force was greater compared to the previous studies but this could be attributed to the varus moment generated during the gait cycle or due to a difference in walking velocity. The previous studies used normal healthy individuals and did not consider varus alignment. Morrison<sup>25</sup> observed that the forces in the knee ligaments varied significantly between individuals due to subject-specific gait characteristics and knee-joint geometry, which is in agreement with our analysis.

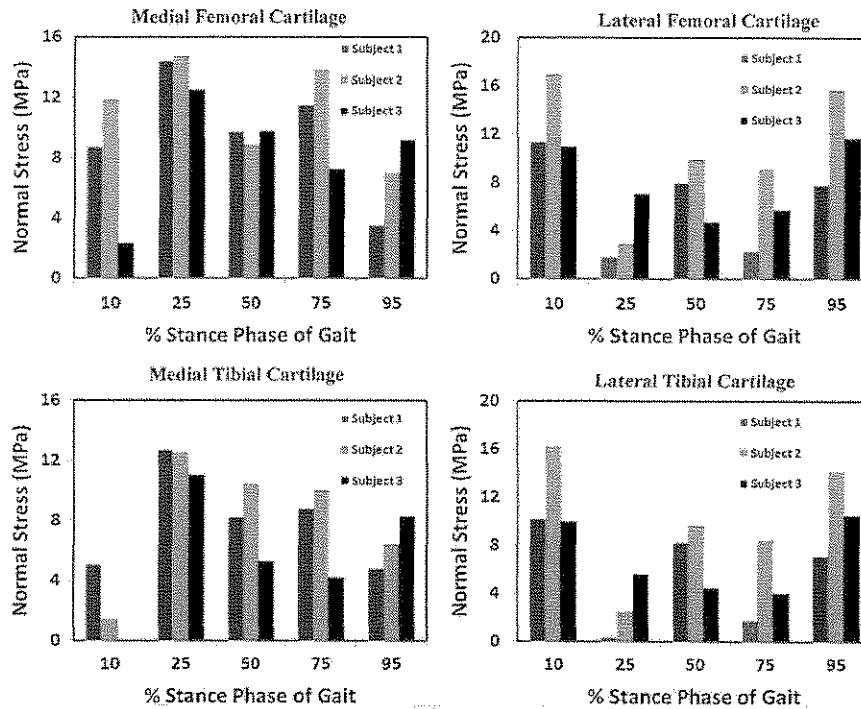
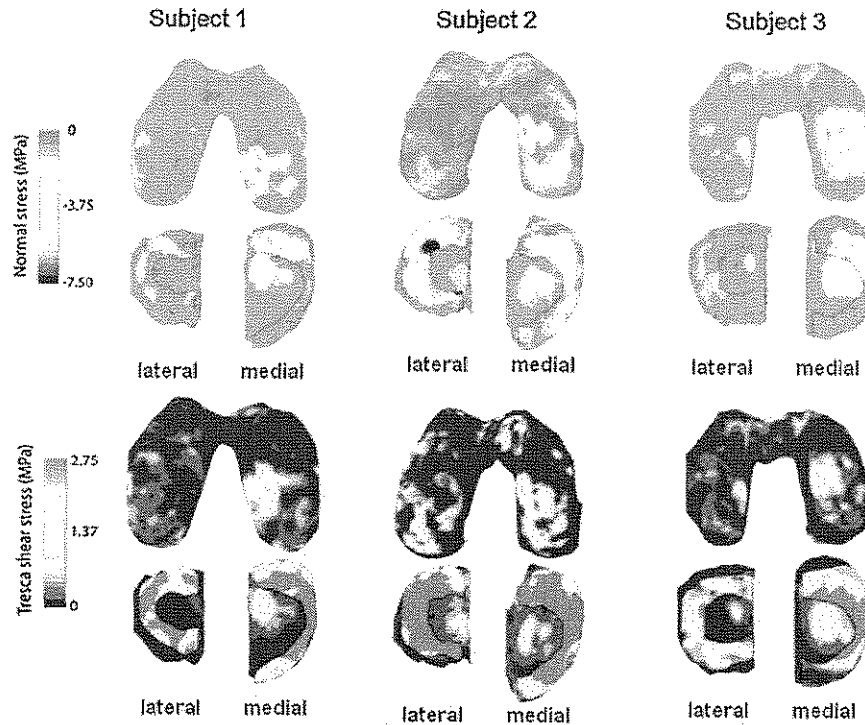


Figure 4. Maximum compressive stress on medial femoral, lateral femoral cartilage, medial tibial cartilage, and lateral tibial cartilage during the stance phase of the gait cycle.

The key limitation of our study is the low number of individuals examined which makes drawing any quantitative and general conclusions infeasible. However, our study provides valuable insight into the role of frontal plane tibiofemoral angle on the stress and strain at the knee and motivates studies with a larger number of individuals using subject-specific models during walking and other functional activities. Furthermore, the dynamic tibiofemoral alignment may be different compared to the static tibiofemoral alignment and monitoring the dynamic alignment may provide further insight into the compartmental loading at the knee joint during gait. Noyes et al.<sup>33</sup> analyzed knee-joint loads and ligament tensile forces in ACL-deficient and varus-aligned individuals during level walking. It was observed that a majority of the subjects exhibited high medial knee compartment loads and high lateral soft tissue loads but it was not correlated with the degree of alignment measured during standing roentgenograms. Monitoring the dynamic tibiofemoral alignment during gait may provide a correlation between the medial compartment knee-joint loading and dynamic tibiofemoral alignment.

The overall muscle-force contributions represent a minimum due to the absence of co-contraction in the reduction model but provides a more realistic loading condition than applying the knee-joint reactions determined from the inverse dynamics analysis alone. To

demonstrate the validity of the current muscle-force reduction model, the peak muscle forces and activation timing (Fig. 1A) was compared to EMG data taken from Besier et al.<sup>34</sup> based on data of 16 pain-free control subjects monitored during normal gait (Table 3). The peak muscle forces and activation timing from Besier et al.<sup>34</sup> are approximations based on graphical data and summation of the different muscles that compose the different muscle groups including the hamstrings [semi-membranosus (SM), semi-tendinosus (ST), and bicep femoris (BF)], quadriceps [vastus medialis (VM), vastus lateralis (VL), vastus intermedius (VI), and rectus femoris (RF)], and the gastrocnemius [lateral gastrocnemius (LG) and medial gastrocnemius (MG)]. Comparison of the current model to EMG data show similar results that are within the standard deviation calculated by Besier et al.<sup>34</sup> A limitation of the current model is it does not take into account the individual recruitment patterns of the different muscles. For example, the quadriceps muscles are composed of four muscles. In the current muscle-force reduction model, the quadriceps act at 20–25% stance phase and at 90–100% of the stance phase. EMG data from Besier et al.<sup>34</sup> showed the quadriceps muscle acting at the same timing, however, they have the ability to show the individual muscle recruitment patterns as the SM, ST, and BF act at 20–25% of the stance phase while the RF acts at toe off (90–100% of the stance phase).



**Figure 5.** Subject-specific finite element results of the compressive stress distribution and Tresca shear stress distribution of the femoral cartilage and tibial plateau (meniscus and tibial cartilage) for Subject 1 (varus), Subject 2 (normal), and Subject 3 (valgus) at approximately 25% of the stance phase of the gait cycle. This was associated with the initial peak varus moment.

Many existing FE studies use unrealistic loading conditions and do not typically consider the knee-flexion angle, which affects the magnitude and location of the maximum stress and strain in the knee cartilage.<sup>10-12</sup> In addition, subject-specific joint geometry is very important as thickness variation and joint architecture could greatly affect the stress and strain distribution in the cartilage. Thus, our subject-specific approach provides valuable insight that previous FE studies could not. It should be noted that in our subject-specific FE models the muscle forces and joint reaction forces are applied at one location in the femur. The actual muscle architecture at the knee is very complicated. The muscle forces at the knee occur at different locations and the magnitude of the muscles vary greatly over the stance phase of the gait cycle. Incorporating the muscle forces based on muscle location and line of action would enhance results

of the actual stress and strain distribution at the knee but may also increase error due to the large number of variables. However, developing the muscle-force data is very difficult and involves complicated models. Furthermore, determining subject-specific muscle data would be very difficult and expensive due to the high cost of MRI plus the multiple views needed from the MRI to determine the size and location of the muscles at the knee. Another consideration is that the muscle forces acted to oppose the external flexion/extension, however, in the current model the LCL was the only component that opposed the varus knee moment and the MCL was the only component that opposed the valgus knee moment. Inclusion of the muscle forces to oppose the varus/valgus moment would have an effect on the overall force distribution to the medial and lateral knee compartments during the stance phase. The stress distribution may

**Table 2.** Finite Element Results for Normalized Maximum Compressive Stress, Normalized Maximum Shear Stress, and the Normal Strain on the Medial Tibial Cartilage and Femoral Cartilage

Subject	Normalized Compressive Stress (MPa/N)		Normalized Tresca Stress (MPa/N)		Normal Strain (%)	
	Tibia	Femur	Tibia	Femur	Tibia	Femur
1 (varus)	0.020	0.023	0.009	0.011	18.66	26.66
2 (normal)	0.017	0.020	0.007	0.010	17.01	20.67
3 (valgus)	0.016	0.018	0.006	0.007	14.99	16.16

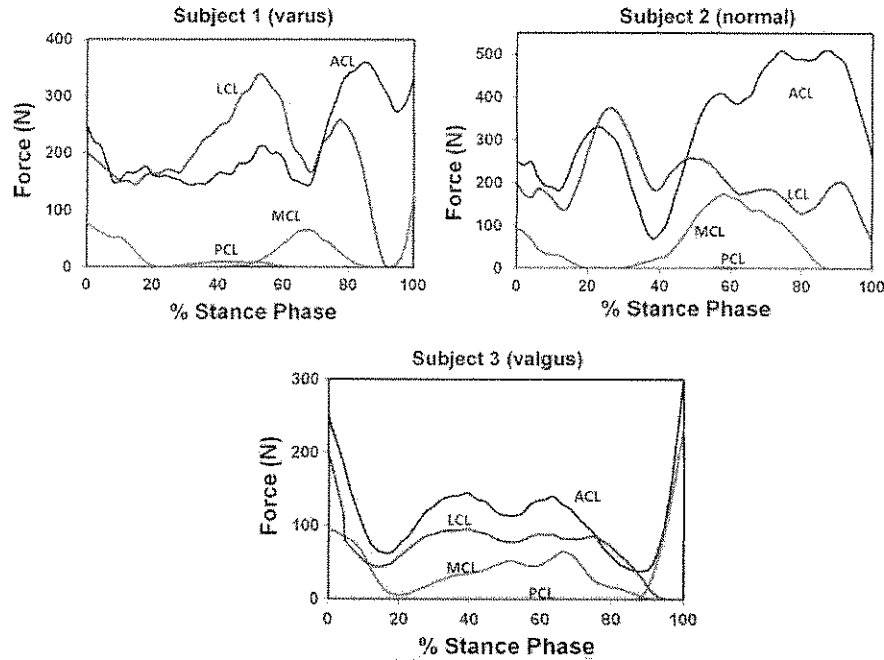


Figure 6. Ligament forces during the stance phase of gait for each of the subjects calculated using finite element analysis.

Table 3. Activation Timing and Peak Force for the Different Muscle Groups From EMG Data From Besier et al. and for the Subjects in Current Study Based on the Muscle-Force Reduction Model

	Muscles Group			
	Hams (SM, ST, BF)	Quads (VM, VI, VL)	Gast (MG, LG)	Quads (RF)
Activation timing, % of stance phase	0–10%	20–25%	70–75%	90–100%
Besier et al. (N) <sup>a</sup>	886	1,087	688	85
Subj. 1 (N)	638	699	470	424
Subj. 2 (N)	1,363	1,319	362	483
Subj. 3 (N)	739	747	743	384

<sup>a</sup>Approximations based on graphical data.

also change and the peak values of the stress and strain may decrease.

The material models used in this investigation were linear elastic. The mechanical properties of the soft tissue at the knee are nonlinear and the material model in this investigation does not account for the effect of loading rate or stress relaxation. This may change the magnitude of the stress and strain but the distribution to the medial compartment would be similar.

In this study, we developed a subject-specific method to determine the stress and strain at the knee cartilage during the stance phase of the gait cycle. The method developed in this study could be used to identify individuals susceptible to OA, assess the effectiveness of OA preventive measures and for long-term follow-up studies. Limitations in this study include the small study population and assumptions (muscle-force model, material model, etc.) in the models. However, this study

provides useful subject-specific data that observes the role of different biomechanical factors on the stress and strain at the knee cartilage.

#### ACKNOWLEDGMENTS

This work was supported in part by the Department of Mechanical and Industrial Engineering, Northeastern University. We thank Dr. Bijan Najafi from Rosalind Franklin University of Medicine and Science and the anonymous reviewers for their constructive comments and suggestions.

#### REFERENCES

1. Felson DT, Zhang Y. 1998. An update on the epidemiology of knee and hip osteoarthritis with a view to prevention. *Arthritis Rheum* 41:1343–1355.
2. Sharma L, Song J, Felson DT, et al. 2001. The role of knee alignment in disease progression and functional decline in knee osteoarthritis. *JAMA* 286:188–195.



3. Karachalios T, Sarangi PP, Newman JH. 1994. Severe varus and valgus deformities treated by total knee arthroplasty. *J Bone Joint Surg* 76:938-942.
4. Johnson F, Leitzl S, Waugh W. 1980. The distribution of load across the knee. *J Bone Joint Surg* 67-B:346-349.
5. Hsu RW, Himeno S, Coventry MB, et al. 1988. Normal axial alignment of the lower extremity and load-bearing distribution at the knee. *Clin Orthop Relat Res* 255:215-227.
6. Andriacchi TP. 1994. Dynamics of knee malalignment. *Orthop Clin North Am* 25:395-403.
7. Sharma L. 2001. Local factors in osteoarthritis. *Curr Opin Rheumatol* 13:441-446.
8. Tetsworth K, Paley D. 1994. Malalignment and degenerative arthropathy. *Orthop Clin North Am* 25:367-377.
9. Andriacchi TP, Mündermann A, Smith RL, et al. 2004. A framework for the in vivo pathomechanics of osteoarthritis at the knee. *Ann Biomed Eng* 32:447-457.
10. Peña E, Calvo B, Martínez MA, et al. 2006. A three-dimensional finite element analysis of the combined behavior of ligaments and menisci in the healthy human knee joint. *J Biomech* 39:1686-1701.
11. Li G, Gil J, Kanamori A, et al. 1999. A validated three-dimensional model of a human knee joint. *J Biomech Eng* 121:657-662.
12. Haut Donahue TL, Hull ML, Rashid MM, et al. 2002. A finite element model of the human knee joint for the study of tibiofemoral contact. *J Biomech Eng* 124:273-280.
13. Andriacchi TP, Briant PL, Beville SL, et al. 2006. Rotational changes at the knee after ACL injury cause cartilage thinning. *Clin Orthop Relat Res* 442:39-44.
14. Li G, Suggs J, Gill T. 2002. The effect of anterior cruciate ligament injury on knee joint function under a simulated muscle load: a three-dimensional computational simulation. *Ann Biomed Eng* 30:713-720.
15. Zielinska B, Haut Donahue TL. 2006. 3D finite element model of meniscectomy: changes in joint contact behavior. *J Biomech Eng* 128:115-123.
16. Peña E, Calvo B, Martínez MA, et al. 2005. Element analysis of the effect of meniscal tears and meniscectomies on human knee biomechanics. *Clin Biomech* 20:498-507.
17. Kirkwood RN, Culham EG, Costigan P. 1999. Radiographic and non-invasive determination of the hip joint center location: effect on hip joint moments. *Clin Biomech* 14:227-235.
18. Horton GA, Reckling FW. 1995. Femoral pulse as a guide to the mechanical axis in total knee arthroplasty. *J Arthroplasty* 10:780-784.
19. Ford KR, Myer GD, Hewett TE. 2003. Valgus knee motion during landing in high school female and male basketball players. *Med Sci Sports Exerc* 35:1745-1750.
20. EVaRT Version 5.0 User's Manual, Motion Analysis Corporation, Santa Rosa, CA.
21. Dubost V, Annweiler C, Aminian K, et al. 2008. Stride-to-stride variability while enumerating animal names among healthy young adults: result of stride velocity or effect of attention-demanding task? *Gait Posture* 27:138-143.
22. Dubost V, Kressig RW, Gonthier R, et al. 2006. Relationships between dual-task related changes in stride velocity and stride time variability in healthy older adults. *Hum Mov Sci* 25:372-382.
23. Beauchet O, Kressig RW, Najafi B, et al. 2003. Age-related decline of gait control under a dual-task condition. *J Am Geriatr Soc* 51:1187-1188.
24. Yang NH, Canayan P, Nayeb-Hashemi H, et al. 2009. Protocol for constructing subject-specific biomechanical model of knee joint. *Comput<sup>AQ3</sup> Methods Biomech Biomed Eng* (in press).
25. Morrison JB. 1970. The mechanics of the knee joint in relation to normal walking. *J Biomech* 3:51-61.
26. Schipplein OD, Andriacchi TP. 1991. Interaction between active and passive knee stabilizers during level walking. *J Orthop Res* 9:113-119.
27. Repo RU, Finlay JB. 1977. Survival of articular cartilage after controlled impact. *J Bone Joint Surg* 59:1068-1076.
28. Chen CT, Bharagava M, Lin PM, et al. 2003. Time, stress and location dependent chondrocyte death and collagen damage in cyclically loaded articular cartilage. *J Orthop Res* 21:888-898.
29. Fregly BJ. 2008. Computational assessment of combinations of gait modifications for knee osteoarthritis rehabilitations. *IEEE Trans Biomed Eng* 55:2104-2106.
30. Dingwell JB, Cusumano JP, Cavanagh PR, et al. 2001. Local dynamic stability versus kinematic variability of continuous overground and treadmill walking. *J Biomech Eng* 123:27-32.
31. Shelburne KB, Torry MR, Pandy MG. 2005. Muscle, ligament, and joint-contact forces at the knee during walking. *Med Sci Sports Exerc* 37:1948-1956.
32. Harrington LJ. 1976. A bioengineering analysis of force actions at the knee in normal and pathological gait. *Biomed Eng* 11:167-172.
33. Noyes FR, Schipplein OD, Andriacchi TP, et al. 1992. The anterior cruciate ligament-deficient knee with varus alignment. *Am J Sports Med* 20:707-716.
34. Besier TF, Fredericson M, Gold GE, et al. 2009. Knee muscle forces during walking and running in patellofemoral pain patients and pain-free controls. *J Biomech* 42:898-905.

AQ3

AQ1: Please check the suitability of the suggested short title.

AQ2: Please provide the Fax no.

AQ3: Please update.